

An upper limit on the electron-neutrino flux from the HiRes detector

R. U. Abbasi,¹ T. Abu-Zayyad,¹ M. Allen,¹ J. F. Amann,² G. Archbold,¹ K. Bebv,¹
 J. W. Belz,³ S. Y. Ben Zvi,⁴ D. R. Bergman,⁵ A. Biesiadecka,⁵ S. A. Blake,¹ J. H. Boyer,⁴
 O. A. Brusova,¹ G. W. Burt,¹ C. Cannon,¹ Z. Cao,¹ W. Deng,¹ Y. Fedorova,¹ J. Findlay,¹
 C. B. Finley,⁴ R. C. Gray,¹ W. F. Hanlon,¹ C. M. Homann,² M. H. Holzschetter,²
 G. Hughes,⁵ P. Huntmeyer,¹ D. Ivanov,⁵ B. F. Jones,¹ C. C. H. Jui,¹ K. Kim,¹ M. A. Kim,³
 B. C. Knapp,⁴ E. C. Loh,¹ M. M. Maestas,¹ N. Manago,⁶ E. J. Mannel,⁴ L. J. Marek,²
 K. Martens,¹ J. A. J. Matthews,⁷ J. N. Matthews,¹ S. A. Moore,¹ A. O'Neill,⁴
 C. A. Painter,² L. Perera,⁵ K. Reil,¹ R. Riehle,¹ M. D. Roberts,⁷ D. Rodriguez,¹
 M. Sasaki,⁶ S. R. Schnetzer,⁵ L. M. Scott,⁵ M. Seman,⁴ G. Sinnis,² J. D. Smith,¹ R. Snow,¹
 P. Sokolsky,¹ C. Song,⁴ R. W. Springer,¹ B. T. Stokes,¹ S. R. Stratton,⁵ J. R. Thomas,¹
 S. B. Thomas,¹ G. B. Thomson,⁵ D. Tupa,² L. R. Wiencke,¹ A. Zech⁵ and X. Zhang⁴

A B S T R A C T

Air- uorescence detectors such as the High Resolution Fly's Eye (HiRes) detector are very sensitive to upward-going, Earth-skimming ultrahigh energy electron-neutrino-induced showers. This is due to the relatively large interaction cross sections of these high-energy neutrinos and to the Landau-Pomeranchuk-Migdal (LPM) effect. The LPM effect causes a significant decrease in the cross sections for bremsstrahlung and pair production, allowing charged-current electron-neutrino-induced showers occurring deep in the Earth's crust to be detectable as they exit the Earth into the atmosphere. A search for upward-going neutrino-induced showers in the HiRes-II monocular dataset has yielded a null

¹University of Utah, Department of Physics and High Energy Astrophysics Institute, Salt Lake City, UT 84112, USA.

²Los Alamos National Laboratory, Los Alamos, NM 87545, USA.

³University of Montana, Department of Physics and Astronomy, Missoula, MT 59812, USA.

⁴Columbia University, Department of Physics and Nevis Laboratories, New York, NY 10027, USA.

⁵Rutgers | The State University of New Jersey, Department of Physics and Astronomy, Piscataway, NJ 08854, USA.

⁶University of Tokyo, Institute for Cosmic Ray Research, Kashiwa City, Chiba 277-8582, Japan.

⁷University of New Mexico, Department of Physics and Astronomy, Albuquerque, NM 87131, USA.

result. From an LPM calculation of the energy spectrum of charged particles as a function of primary energy and depth for electron-induced showers in rock, we calculate the shape of the resulting profile of these showers in air. We describe a full detector Monte Carlo simulation to determine the detector response to upward-going electron-neutrino-induced cascades and present an upper limit on the flux of electron-neutrinos.

Subject headings: cosmic rays | neutrinos | acceleration of particles | large-scale structure of the universe

1. Introduction

We report on a search for upward-going electron-neutrino showers in the High-Resolution Fly's Eye II data set, and on the upper limit on the flux of ν_e set by the HIRes-II detector. The HIRes project has been discussed previously (Abu-Zayyad et al. 1999; Boyer et al. 2002); the detector is an air-fluorescence detector located on two sites 12.6 km apart in Utah at the U.S. Army Dugway Proving Ground. The HIRes-II detector, located on Camel's Back Ridge, is composed of 42 spherical mirrors of 3.7 m^2 effective area covering nearly 360° in azimuth. Half of these, known as ring-one mirrors, cover between 3° - 17° in elevation; the other half (ring-two) cover between 17° - 31° in elevation.

Cosmogenic neutrinos, with energies mostly in excess of 10^{18} eV , are produced via and π decays following photopion production from high-energy cosmic ray protons incident on the cosmic microwave background radiation (Stecker 1968; Margolis et al. 1978). There is evidence to suggest that gamma-ray bursts and active galactic nuclei jets are possible sources of high-energy cosmic rays and neutrinos (Waxman & Bahcall 1997; Halzen & Zas 1997). Several theoretical limits on the flux of cosmogenic neutrinos have been proposed (Semikoz & Sigl 2004; Seckel & Stanev 2005).

Although large uncertainties exist, neutrino cross sections have been calculated to vary from $\sim 10^{-32} \text{ cm}^2$ at 10^{18} eV to $\sim 10^{-31} \text{ cm}^2$ at 10^{21} eV (Reno 2005). The opacity of the earth to neutrinos at these high energies therefore prohibits the detection of any upward-going event with an elevation angle larger than a few degrees.

In the charged-current interaction of a ν_e in the earth's crust, a high-energy electron will be created. The electromagnetic cascade generated by the electron will develop much more slowly due to the onset of the Landau-Pomeranchuk-Migdal (LPM) effect. The LPM effect, first described classically by Landau & Pomeranchuk (1953) and later given a quantum-mechanical treatment by Migdal (1956), predicts that the cross sections for bremsstrahlung

and pair-production should decrease for a high-energy charged particle propagating in a dense medium, effectively slowing and elongating the development of the resulting shower of particles (a detailed, more modern approach can be found in Takahashi et al. (2003) and Baier & Katkov (2004)). The energy at which this effect becomes appreciable is inversely proportional to the square of the Lorentz factor γ , and therefore the LPM effect should be much more pronounced for the showers generated from a ν_e charged-current interaction than for showers precipitated by μ or τ in the energy range in which HIRes is sensitive.

It is most probable that a neutrino-induced electromagnetic cascade would be long and nearly-horizontal and observed primarily in the HIRes-II ring-one mirrors. Due to the LPM effect, one expects electron-neutrino-induced showers that begin several tens to hundreds of meters deep in the crust to emerge with enough charged particles to be detected by HIRes-II, thereby increasing the effective aperture of the detector at high energies.

2. Search for upward-going neutrino events

The entire HIRes-II data set, which extends from late 1999 to Spring 2006, was considered when searching for evidence of neutrino-induced upward-going showers. Using the standard routines that were developed for analyzing downward-going cosmic-ray events, we reconstructed the trajectories of each upward-going event based on the measured timing and geometry (see Sokolsky (1989) for a description of time- and plane-fitting for extensive air showers).

The data were then filtered in time and position to exclude all calibration laser events, which resulted in a loss in the detector aperture of less than 1%. Additionally and consistent with standard procedure for the analysis of cosmic-ray data, events were rejected that passed within 100 meters of the detector, had track lengths smaller than 10 μ , and that had geometrical uncertainties from timing greater than 36 μ .

3. The Landau-Pomeranchuk-Migdal Effect

At electron energies below the LPM threshold energy ($61.5 L_{cm}$ TeV (Stanev et al. 1982), where L_{cm} is the interaction length in cm), the longitudinal profile of an electromagnetic shower can be well approximated by the relation

$$N(t) = \frac{0.31}{t^{1.2}} \exp\left(-t - \frac{3}{2} \ln t\right) \quad (1)$$

This functional form was first described by Greisen (1956), with \ln_0 as the log of the ratio of the energy of the incident electron to its critical energy E_c , t as the depth in radiation lengths and $s = \frac{3t}{[t+2 \ln_0]}$.

This relation begins to break down at high energies, greatly underestimating the distance over which the electromagnetic cascade evolves due to the decrease in the cross sections for bremsstrahlung and e^+e^- pair production. Studies of the electron shower profiles in rock, water and lead above the LPM threshold energy have been conducted previously (Misaki 1990; Stanev et al. 1982; Alvarez-Muniz 1999). As expected, the results of these analyses show that the shower profiles of electron-induced cascades are elongated significantly with respect to the Greisen approximation at energies above the LPM threshold, and evolve differently based on the densities of the media in which the showers propagate.

4. Calculation of sensitivity to electron-neutrino showers

To simulate ν_e -induced electromagnetic cascades, we used a four-step process. First, we calculated the average profiles of electron-induced showers using the LPM effect. We then used a Monte Carlo method to simulate the arrival directions and interaction points of ν_e around the HiRes detector. The shower profiles in air were then passed into the HiRes detector Monte Carlo to calculate the amount of light seen by the detector. The HiRes analysis programs were then run on the resulting Monte Carlo events to arrive at a ν_e aperture.

4.1. Calculating electron-neutrino-induced electromagnetic cascade profiles

In order to treat charged-current $\nu_e N$ interactions in the earth's crust, it is necessary to understand the physics of the transition of an electromagnetic cascade from a dense medium to a less dense medium (namely, from rock to air). It is therefore important not only to know the number of charged particles after traversal of a given amount of material in rock, but also the energy spectrum of these particles as they leave the ground and enter the atmosphere.

We followed the formalism of Stanev et al. (1982) for calculating the energy-dependence of the probabilities for undergoing pair production and bremsstrahlung at LPM energies. Taking into account any other losses (e.g. Compton scattering and ionization energy loss), we calculated two functions: $N_e^{\text{rock}}(E_0; E; d)$ and $N_e^{\text{air}}(E_0; E; d)$, which describe the average number of charged particles with energy E resulting from the cascade of an electron, positron or photon with initial energy E_0 after traversing an amount of material X in rock or air. The

functions N_e^{rock} and N_e^{air} were determined for E_0 at every decade between 10^{12} and 10^{21} eV using our LPM calculation and from E_c to 10^{12} eV using Equation 1; LPM calculations of shower profiles from particles with initial energies below 10^{12} eV were found to be nearly identical to profiles calculated using Equation 1.

4.2. Simulating neutrino events

We approximated the earth as a sphere with a radius equal to that at the Dugway Proving Ground in Utah. The density below 58.4 km beneath the surface (mantle) and the density from 58.4 km to the surface (crust) were taken to be 4.60 and 2.80 g cm^{-3} respectively. The atmosphere was also simulated up to a height of 50 km above sea level.

Electron-neutrino energies were considered from $\log E$ of 18 to 21. The energy-dependence and inelasticity of the charged- and neutral-current $\bar{\nu}_e$ interaction cross sections were calculated based on the pQCD CTEQ5 model (Lai et al. 2000; Gazizov & Kowalski 2005). From the ratio of the cross sections for charged-current (CC) and neutral-current (NC) interactions, 70% of the events were thrown as CC events, while the remaining 30% were considered NC events.

Neutrino arrival directions were chosen at random such that they only penetrated the atmosphere no more than 15° below the horizon. Events with elevation angles greater than 15° do not contribute appreciably to the Hires-II total $\bar{\nu}_e$ aperture due to the very small probability of their transmission through the crust and mantle and subsequent interaction near the detector (a 10^{18} eV neutrino at 15° has a probability of 10^{-12} of transmission and interaction near the detector; this value drops to 10^{-60} at 10^{21} eV). The variables describing the geometry of the neutrino trajectory were determined, such as the distance of closest approach to the detector, the vector normal to the shower-detector plane, and the angle of the shower in the shower-detector plane.

For these earth-skimming events, the traversal of a critical amount of material X_c (measured in g cm^{-2}) was found such that when the shower emerges from the rock into air, it contains at least 10^7 charged particles; showers with a maximum number of charged particles less than 10^7 will not trigger the Hires detector. This critical path length is used to separate the probabilities for neutrino transmission and interaction. The transmission probability t_r was calculated as the probability for a neutrino to penetrate up to X_c . The interaction probability i_r was calculated from the path length of the neutrino from X_c until escape from the atmosphere. Since the amount of material traversed in the interaction region is always much less than the mean neutrino interaction length, the actual point of interaction for each neu-

trino was then chosen at random for distances $X < X_c$. For neutrinos with small elevation angles that do not pass through the Earth, we considered events that entered the atmosphere above the horizon as well as those that interacted below the horizon and yielded at least 10^7 particles at the horizon. For events interacting below the horizon, X_c was taken to be the amount of air penetrated at the horizon. In the case of events that entered the atmosphere above the horizon, we set t to unity and calculated i from the total distance traversed in the atmosphere.

For all eN interactions the energy transferred to the secondary electron or hadron was chosen from the inelasticity distribution ($d = dy$) for the pQCD CTEQ5 model. For Earth-skimming CC events, the resulting observable profile in air was found from a superposition of showers obtained from the energy spectrum of electrons, positrons and photons emerging from the rock. The profiles of CC events that did not pass through the earth were interpolated from the N_e^{air} functions described in the previous section. The profiles for all NC events were calculated using the standard Gaisser-Hillas model (Gaisser 1990). Each profile was then weighted by a factor $w = t i$, to describe the total probability of transmission and interaction near HIRes-II. Figure 1 shows the average profiles of ve electron-induced air showers emerging from the ground at different depths along an average 10^{20} eV electron-induced shower in rock.

4.3. Simulating detection by HIRes

Having generated shower profiles using the LPM effect, the shower profiles were then passed through a HIRes Monte Carlo program which models the response of the detector to cosmic-ray-induced showers. This program determines the amount of fluorescence and Cerenkov photons produced for a given number of charged particles, and scatters and attenuates the light appropriately when given the known variables describing the geometry of the shower with respect to the detector. The program then models the HIRes-II trigger conditions to decide if the simulated shower is read out by the detector (Abbasi et al. 2004).

4.4. Analysis and filtering of simulated events

Simulated showers which triggered the detector were analyzed using the same routines used in the analysis of the real data used in our search for neutrinos in the upward-going HIRes-II data. The variables describing the geometry of the shower were t and compared to the known variables. An event was considered accepted when it passed the same cuts

described in Section 2.

5. Calculating an electron-neutrino flux upper limit

For the purposes of arriving at a predicted H iRes-II ν_e aperture, the simulated events were collected in 30 0.1-decade energy bins from 10^{18} to 10^{21} eV. The aperture for a given energy bin was found

$$(A)_{\nu_e} = 2 \int_0^{\pi/30} \sin(\theta) d\theta R^2 \frac{P_{N_A}!}{N_T} \quad (2)$$

where R is the radius of the earth extended 50 km to the edge of the atmosphere. The geometrical component of the aperture is derived from the area and solid angle of a 30 cap on a sphere of radius R . This is then adjusted by the weighting factor w (discussed in Section 4.2) for each of the N_A events that trigger the detector out of a total N_T events thrown in the given energy bin. The H iRes-II ν_e aperture is shown in Figure 2.

Consistent with our study of (Martens 2007), we calculate a flux limit in three energy bins: $E = 10^{18}, 10^{19}, 10^{19} - 10^{20}$, and $10^{20} - 10^{21}$ eV, over the total H iRes lifetime of 3638 hours. We observe no neutrino events over the entire energy range. We calculate the flux limit ($E^2 \frac{dN}{dE}$) at the 90% confidence level to be $4.06 \cdot 10^3, 3.55 \cdot 10^3$ and $4.86 \cdot 10^3$ eV $\text{cm}^{-2} \text{sr}^{-1} \text{s}^{-1}$ at $10^{18.5}, 10^{19.5}$ and $10^{20.5}$ eV, respectively. Combined with our results and provided equal mixing of all neutrino flavors, this reduces the limit to $3.81 \cdot 10^2, 9.73 \cdot 10^3$ and $4.71 \cdot 10^3$ eV $\text{cm}^{-2} \text{sr}^{-1} \text{s}^{-1}$.

6. Discussion

As is the case with all high-energy neutrino calculations, the largest uncertainty lies in the extrapolation of N cross sections. Different cross section models can cause the limits to vary somewhat. The incorporation of cross sections from previous and more recent versions of the CTEQ model can change the limits by as much as 10 to 40% at the lowest and highest energies, respectively.

Recent work imposing the Froissart bound on structure functions for extrapolating N cross sections show a decrease in cross sections at 10^{21} eV by about a factor of 8 over the CTEQ 5 parameterization (Block 2007). These cross sections increase our ν_e limit by 40% at the lowest energy bin and increase the value of our highest energy bin by a factor of 3.

In addition to uncertainties in N cross sections, our limits are also sensitive to the energy transferred to the secondary electron or hadron. From parameterizations of the mean inelasticity in N interactions (Quigg et al. 1986), if we allow the transfer of exactly 80% of the neutrino energy to the electron (and 20% to the hadron), our ϕ_e limits will increase between about 15% at $10^{18.5}$ eV, remain unchanged in the middle energy bin and decrease by about 5% at $10^{21.5}$ eV.

7. Conclusion

We have found no evidence of upward-going neutrino-induced cosmic-ray showers in the HiRes-II data. We have presented a technique for modeling the full HiRes-II detector response to ultrahigh energy neutrino-induced LPM cascades in rock and air. With no neutrino events seen in the HiRes-II data, and provided equal mixing of all neutrino flavors, we have found an upper limit on the flux of ultrahigh energy neutrinos at a 90% confidence limit.

Figure 3 shows the upper limit on the neutrino flux from the analysis of the HiRes ϕ_e and ϕ_h flux limits as compared to three theoretical curves and to calculated flux limits from other experiments. The ϕ_e flux limits reported here have improved upon those for the Fly's Eye by about two and a half orders of magnitude. Combined with the results of the analysis, this limit lies just above the theoretical neutrino flux of Semikoz & Sigl (2004), and about an order of magnitude above that of Seckel & Stanev (2005). Our combined neutrino flux limit is about two and a half orders of magnitude above the cosmogenic neutrino flux predictions of Brusova (2007), which has been derived from a proton injection model with cosmologically evolving sources and injection spectra that fit the HiRes cosmic-ray spectrum.

We would like to thank Steve Barwick for useful discussions and recommendations while writing this paper. This work was supported by US NSF grants PHY-9100221, PHY-9321949, PHY-9322298, PHY-9904048, PHY-9974537, PHY-0073057, PHY-0098826, PHY-0140688, PHY-0245428, PHY-0305516, PHY-0307098, PHY-0649681, and PHY-0703893, and by the DOE grant FG03-92ER40732. We gratefully acknowledge the contributions from the technical staffs of our home institutions. The cooperation of Colonels E. Fischer, G. Harter and G. Olsen, the US Army, and the Dugway Proving Ground staff is greatly appreciated.

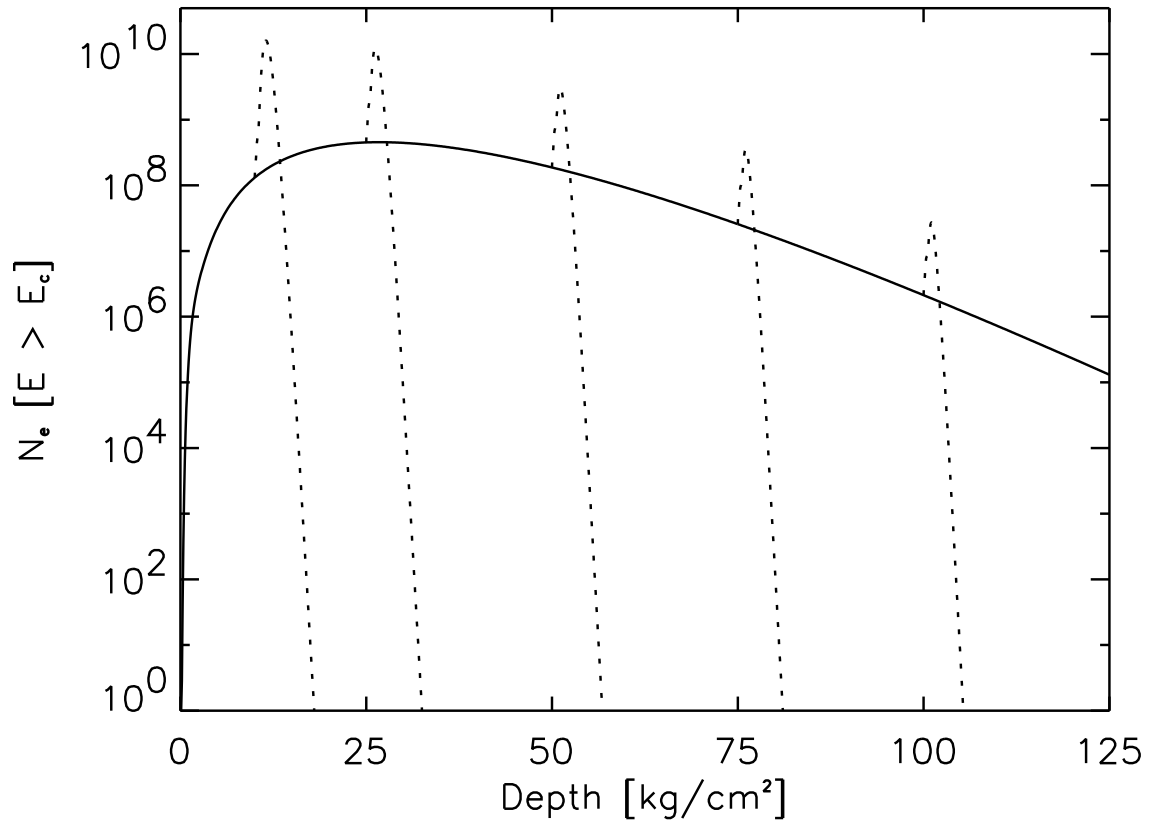


Fig. 1. | An average 10^{20} eV electron shower profile in rock (solid line) with average shower profiles for air showers emerging from the ground at depths of 10000, 25000, 50000, 75000, and 100000 g/cm^2 (dashed lines).

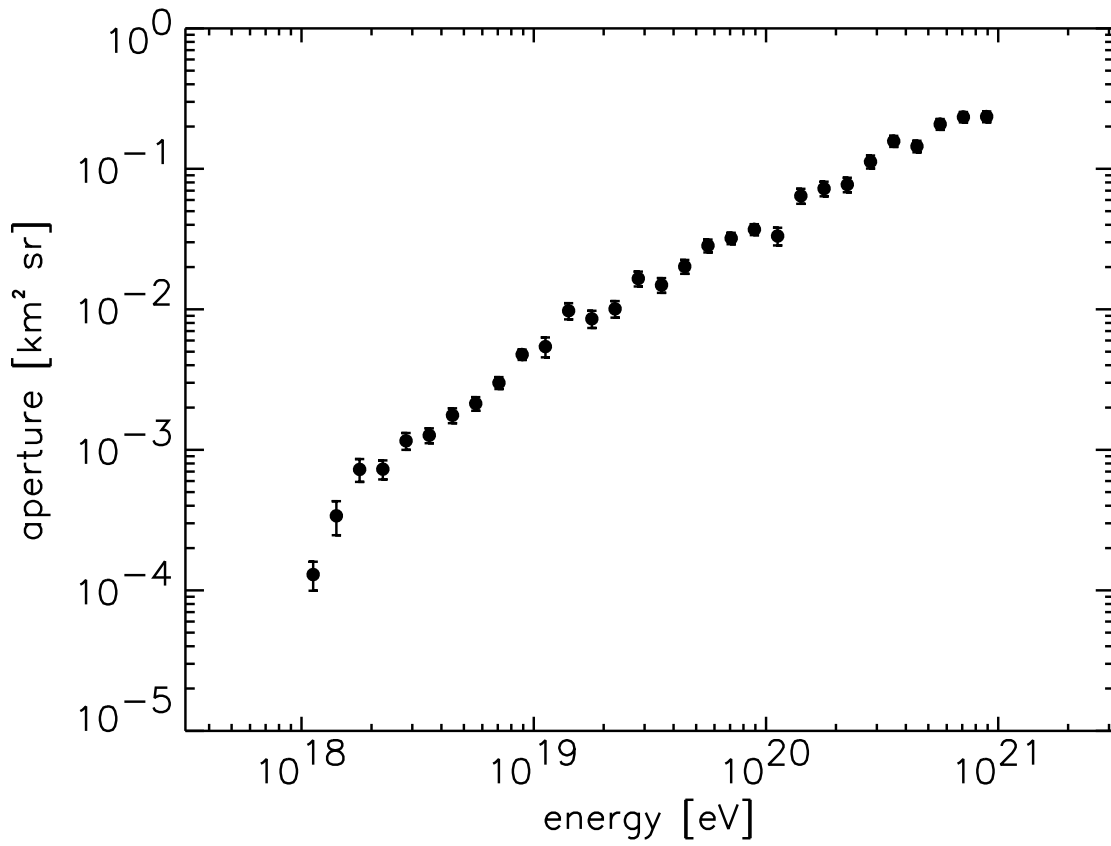


Fig. 2. | The calculated HIRes-II electron-neutrino aperture.

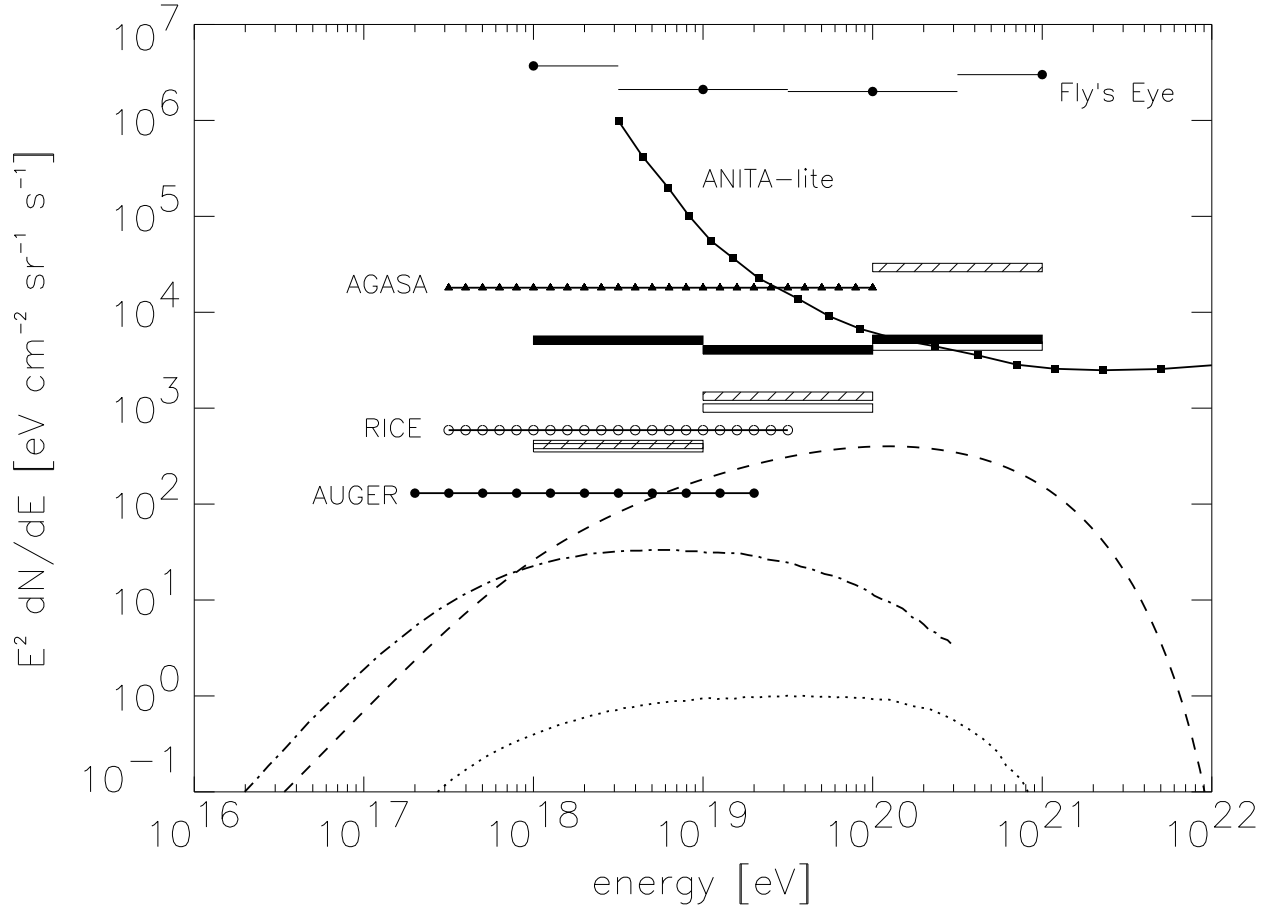


Fig. 3. | The HiRes-II neutrino flux limit. black boxes: ν_e limit (this work). cross-hatched boxes: ν_e limit (Martens 2007). open boxes: ν_e and ν_μ combined flux limit. Dotted line: cosmogenic pavor neutrino flux limit from fits to HiRes cosmic-ray data (Brusova 2007). Dashed line: cosmogenic pavor neutrino flux limit derived from fits to existing cosmic- and gamma-ray data (Semikoz & Sigl 2004). Dot-dashed line: cosmogenic pavor neutrino flux from fits to HiRes and AGASA cosmic-ray data (Seckel & Stanev 2005). Also shown are calculated neutrino flux limits from the Fly's Eye (Baltrusaitis et al. 1984, 1985), ANITA-lite (Gorham et al. 2004), RICE (Kravchenko et al. 2006), AGASA (Chikawa et al. 2001) and Auger (Abraham et al. 2008) experiments.

R E F E R E N C E S

- Abbasi, R . U . , et al. 2004, *Phys. Rev. Lett.*, 92 (15), 151101
- Abraham , J. , et al. 2008, to appear in *Phys. Rev. Lett.*
- Abu-Zayyad, T . , et al. 1999, *Proc. 26th Internat. Cosmic Ray Conf. (Salt Lake City)*, 349
- Alvarez-M uniz, J. 1999, *Proc. 26th Internat. Cosmic Ray Conf. (Salt Lake City)*, 506
- Baier, V . N . & Katkov, V . M . 2004, *Phys. Lett. A* , 327, 202
- Baltrusaitis, R . , Cady, R . , Cassidy, G . , Elbert, J. W . , Gerhardy, P . , Loh, E . , Mizumoto, Y . , Sokolsky, P . & Steck, D . 1984, *ApJ*, 281, L9
- Baltrusaitis, R . M . , Cassidy, G . L . , Elbert, J. W . , Gerhardy, P . R . , Loh, E . C . , Mizumoto, Y . , Sokolsky, P . & Steck, D . 1985, *Phys. Rev. D* , 31, 2192
- Block, M . M . 2007, private communication
- Boyer, J. H . , Knapp, B . C . , Manne, E . J. & Sem an, M . 2002, *Nucl. Inst. Meth.*, A 482, 457
- Brusova, O . A . , et al. 2007, *Proc. 30th Internat. Cosmic Ray Conf. (Merida)*
- Chikawa, M . , et al. 2001, *Proc. 26th Internat. Cosmic Ray Conf. (Hamburg)*, 1142
- Gaisser, T . K . 1990, *Cosmic Rays and Particle Physics* (Cambridge, U . K . : Cambridge University Press)
- Gazizov, A . & Kowalski, M . 2005, *Comp. Phys. Comm.*, 172, 203
- Gorham , P. W . , Hebert, C . L . , Liewer, K . M . , Naudet, C . J . , Saltzberg, D . and Williams, D . 2004, *Phys. Rev. Lett.*, 93 (4), 041101
- Greisen, K . 1956, *Progress in Cosmic Ray Physics*, J. G . Wilson, Amsterdam , Netherlands.
- Halzen, F . & Zas, E . 1997, *ApJ*, 488, 669
- Kravchenko, I. et al. 2006, *Phys. Rev. D* , 73 (8), 082002
- Lai, H . L . , Huston, J . , Kuhlmann, S . , Mor n, J . , Olness, F . , Owens, J. F . , Pumphlin, J . & Tung, W . K . 2000, *European Phys. J. C* , 12, 375
- Landau, L . & Pomeranchuk, I. 1953, *Dok. Akad. Nauk SSSR* , 92, 535
- Margolis, S. H . , Schramm , D . N . & Silberberg, R . 1978, *ApJ*, 221, 990

- Martens, K., et al. 2007, Proc. 30th Internat. Cosmic Ray Conf. (Merida)
- Migdal, A. B. 1956, Phys. Rev., 103, 1811
- Misaki, A. 1990, Il Nuovo Cimento, 13C (4), 733
- Quigg, C, Reno, M. H. & Walker, T. P. 1986, Phys. Rev. Lett., 57, 774
- Reno, M. H. 2005, Nucl. Phys. B Proc. Suppl., 143, 407
- Seckel, D. & Stanev, T. 2005, Phys. Rev. Lett., 95 (14), 141101
- Semikoz, D. V. & Sigl, G. 2004, J. Cosmology and Astro-Particle Physics, 4, 3
- Sokolsky, P. 1989, Introduction to Ultrahigh Energy Cosmic Ray Physics (Redwood City, California: Addison-Wesley Publishing Company, Inc.)
- Stanev, T., Vankov, C., Stenmatter, R. E., Ellsworth, R. W. & Bowen, T. 1982, Phys. Rev. D, 25, 1291
- Stecker, F. W. 1968, Phys. Rev. Lett., 21, 101
- Takahashi, N., Polityko, S., Konishi, E., Kochanov, A., Galkin, V. & Misaki, A. 2003, Proc. 28th Internat. Cosmic Ray Conf. (Tsukuba), 519
- Waxman, E. & Bahcall, J. 1997, Phys. Rev. Lett., 78 (12), 2292